

A 20-kW DC Oak Ridge Converter with Integrated AC & DC Sources for Grid Services and Energy Storage Systems

Erdem Asa¹, Omer C. Onar¹, Rong Zeng¹, Veda P. Galigekere¹, Gui-Jia Su¹, Burak Ozpineci¹, and Kerim Colak²

¹Oak Ridge National Laboratory, National Transportation Research Center, Tennessee, USA

²Hevo Power Inc., New York, USA

E-mail: asae@ornl.com

Abstract— This paper proposes a wireless power transfer (WPT) platform with integrated energy conversion that has the capability for 1) recharging the energy storage systems (ESSs) from the grid systems, including renewable energy sources such as wind, solar, etc., 2) off grid systems recharging the ESSs from dc grid systems, 3) grid recharging of electric vehicles (EVs), and 4) off grid recharging of EVs from ESSs. The unique aspect of the method is the use of multi-interface power electronic converter for the grid and ESSs and EVs that can support a range of applications with ac / dc and dc / dc energy conversion ability in a single converter system. The key enabling technology to achieve these functionalities is Oak Ridge Converter (ORC) with polyphase coupler coil system both developed at ORNL. This new technology enables higher power density WPT systems while allowing the coils to interface from ac grid at 60 Hz frequency or dc source directly merging with 85 kHz operating frequency of switching component. The experimental results of the proposed system are presented for 20 kW output power with the system overall efficiency around 95.4% from dc source and 93% overall efficiency from ac grid achieving 9-10% current total harmonic distortion (THD) and 0.98-0.99 power factor (PF).

Keywords— *Oak Ridge Converter, resonant, high frequency, wireless power transfer, grid, energy storage*

I. INTRODUCTION

Battery energy storage systems (ESSs) can be used as a buffer between the grid and the EV charging systems to reduce

This manuscript has been authored by Oak Ridge National Laboratory, operated by UT-Battelle, LLC, under Contract No. DE-AC05-00OR22725 with the U.S. Department of Energy. The United States Government retains and the publisher, by accepting the article for publication, acknowledges that the United States Government retains a non-exclusive, paid-up, irrevocable, world-wide license to publish or reproduce the published form of this manuscript, or allow others to do so, for United States Government purposes. The Department of Energy will provide public access to these results of federally sponsored research in accordance with the DOE Public Access Plan (<http://energy.gov/downloads/doe-public-access-plan>).

peak demand, facilitate a more levelized demand profile, and are expected to be a critical component of integration of renewables into a stable grid [1], [2]. The high cost of current battery technology is a serious barrier for widespread adoption [3]-[4]. Technological advances which can improve battery utilization can make investment in such systems more attractive. A mobile autonomous energy storage system (MAESS) can improve the utilization of battery energy storage system by supporting the highest output power sources on demand and simplify the problem of adding additional capacity to the distribution system by minimizing the grid disruptions [5], [6].

The availability of mobile recharging system has the potential to drastically reduce range anxiety which is a key impediment to more widespread adoption of pure EVs [7]-[9]. While grid support in the context of renewable energy integration is possible, a fleet of MAESS could be deployed in disaster relief applications to form pop-up microgrids [10]. This functionality may also be of interest for military applications.

ORNL's patented technology Oak Ridge Converter (ORC) [11] and polyphase WPT system will enable a highly integrated ac grid and dc source system. Compared to state of the art, a polyphase WPT coupler system significantly increases the surface power density, reduce the field emissions by half, and provides at least a 50% reduction in dc bus filtering components [12]. Additionally, ORC power electronics architecture can provide energy conversion from the ac grid or from a dc source without any front-end power electronics. It also reduces the cost of the system infrastructure, and the overall complexity. This study presents a 20 kW ac/dc and dc/dc WPT interface system for grid and battery energy storage applications. The topology is explored, operating principles are explained, and theoretical evaluation of the converter is performed. From the grid ac source, the input power factor of 0.98-0.99 is achieved and input current THD level remained around 910%, and the proposed system achieved 93% ac-to-dc efficiency and 95.4% dc-to-dc efficiency.

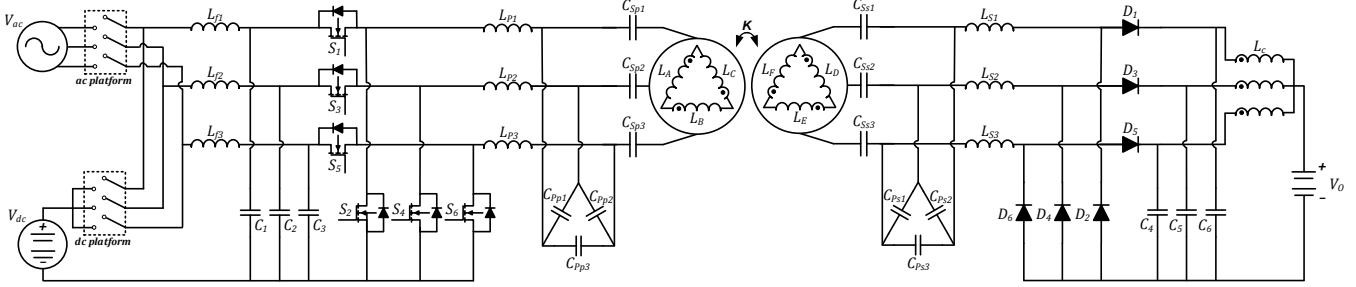


Fig. 1. The proposed integrated WPT system architecture with ac or dc grid connectivity at the input and a dc ESS at the output.

II. THE PROPOSED INTEGRATED WIRELESS POWER TRANSFER PLATFORM

The proposed integrated WPT platform is displayed in Fig. 1. This design enables transferring power from grid to the energy storage or electric vehicle battery. Additionally, this construction delivers charge to the energy storage or electric vehicle battery wirelessly from dc grid or mobile ESSs.

As presented in the schematic, the proposed mechanism converts the 60 Hz ac input or dc input into high-frequency (~85 kHz) ac voltage without using a front-end rectifier with power factor correction (PFC). The proposed structure utilizes a three-phase filter inductor and three input decoupling capacitors, three phase-leg power modules, three-phase LCC - LCC resonant network circuit, a pair of delta connected three-phase couplers, a three-phase diode bridge rectifier, output decoupling capacitor, a common mode choke, and battery load. The high frequency operation is superimposed through LCC - LCC resonant network and couplers to the output rectifier. Then, the signal is rectified through the output decoupling capacitors and common mode choke to the output load. The single-phase circuit representation with resonant tuning network and couplers is shown in Fig. 2.

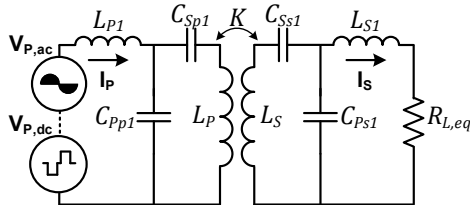


Fig. 2. Single-phase corresponding circuit representation.

For ac grid source, input phase to neutral voltages v_{an} , v_{bn} , and v_{cn} of the proposed coupler structure can be regarded as a three-phase balanced circuit with the input phase voltage rms values in the time domain as,

$$v_{an}(t) = \sqrt{2}V_{an,rms}\sin(2\pi f_{60}t), \quad (1)$$

$$v_{bn}(t) = \sqrt{2}V_{bn,rms}\sin\left(2\pi f_{60}t + \frac{2\pi}{3}\right), \quad (2)$$

$$v_{cn}(t) = \sqrt{2}V_{cn,rms}\sin\left(2\pi f_{60}t - \frac{2\pi}{3}\right) \quad (3)$$

where f_{60} is 60 Hz fundamental grid frequency. The circuit input phase currents i_a , i_b , and i_c can be expressed by the input current rms values in time domain considering the presented converter can reach unity power factor,

$$i_a(t) = \sqrt{2}I_{a,rms}\sin(2\pi f_{60}t), \quad (4)$$

$$i_b(t) = \sqrt{2}I_{b,rms}\sin\left(2\pi f_{60}t + \frac{2\pi}{3}\right), \quad (5)$$

$$i_c(t) = \sqrt{2}I_{c,rms}\sin\left(2\pi f_{60}t - \frac{2\pi}{3}\right). \quad (6)$$

The input phase voltage $v_{P,ac}$ can be calculated as,

$$v_{P,ac}(t) = \frac{2}{\pi}V_{an,rms}\sin(2\pi f_{60}t)\sum_{n=1,3,\dots}^{\infty} \frac{1}{n}\sin(n2\pi f_{sw}t) \quad (7)$$

where f_{sw} is the operating frequency of the converter. Considering the presented system is balanced, the equivalent input phase voltage magnitude $V_{P,ac}$ and the input phase current in the resonant tank, $I_{P,ac}$, can be evaluated as,

$$V_{P,ac} = \frac{2}{\pi\sqrt{2}}V_{ph}, \quad I_{P,ac} = \frac{\pi\sqrt{2}}{2} \frac{P_O}{V_{ph}\eta_{ac}} \quad (8)$$

where V_{ph} reflects the equivalent input phase voltage amplitude V_{ph} ($=V_{an,rms}=V_{bn,rms}=V_{cn,rms}$), P_O is the output power, and η_{ac} is the proposed converter efficiency from ac grid source.

For dc grid source, V_{dc} , the single phase resonant tank voltage amplitude $v_{P,dc}$ and the rms value of $V_{P,dc}$ can be specified as,

$$v_{P,dc}(t) = \frac{2}{\sqrt{3}}V_{dc}\left[\cos(\omega t)dt - \frac{1}{6}\cos(3\omega t)dt\right] \quad (9)$$

$$V_{P,dc} = \frac{5}{3\sqrt{6}}V_{dc} \quad (10)$$

The resonant tank input phase current can be determined as,

$$I_P = \frac{3\sqrt{6}}{5} \frac{P_O}{V_{dc}\eta_{dc}} \quad (11)$$

where η_{dc} is the proposed converter efficiency from dc grid source. In the matrix form, the coupler primary and secondary inductances L_P , L_S can be revealed as,

$$L_P = \begin{bmatrix} L_A & M_{AB} & M_{CA} \\ M_{AB} & L_B & M_{BC} \\ M_{CA} & M_{BC} & L_C \end{bmatrix}, \quad L_S = \begin{bmatrix} L_D & M_{DE} & M_{FD} \\ M_{DE} & L_E & M_{EF} \\ M_{FD} & M_{EF} & L_F \end{bmatrix} \quad (12)$$

where L_A, L_B, L_C are primary side self-inductances and L_D, L_E, L_F are secondary side self-inductances. Also, primary M_{AB}, M_{BC}, M_{CA} and secondary M_{DE}, M_{EF} , and M_{FD} represent mutual inductances between primary phases L_A and L_B , L_B and L_C , L_C and L_A , and secondary phases L_D and L_E , L_E and L_F , L_F and L_D , respectively. With the coupling factor of K between primary and secondary coils, the coupler magnetizing L_M and leakage inductances L_{Lp} and L_{Ls} can be found as,

$$\begin{aligned} L_M &= K\sqrt{L_P L_S}, \quad L_{Lp} = L_P - L_M \text{ and} \\ L_{Ls} &= L_S - L_M \end{aligned} \quad (13)$$

The secondary side output load resistance $R_{L,eq}$ can be attained as,

$$R_{L,eq} = \frac{2V_o^2}{3P_o} \quad (14)$$

In a matrix form equation, the primary and secondary resonant network voltages can be expressed by,

$$\begin{bmatrix} V_P \\ V_O \end{bmatrix} = \begin{bmatrix} j\omega L_{P1} + \left[\frac{1}{j\omega C_{Pp1}} / \left(\frac{1}{j\omega C_{Sp1}} + j\omega L_{L,p} + j\omega L_M \right) \right] \\ -j\omega L_M \\ j\omega L_M + \frac{1}{n^2} \left[j\omega L_{L,s} + \frac{1}{j\omega C_{Ss1}} + \left(\frac{1}{j\omega C_{Ps1}} / j\omega L_{S1} \right) \right] \end{bmatrix} \begin{bmatrix} I_P \\ I_S \end{bmatrix} \quad (15)$$

where V_P indicates $V_{P,ac}$ or $V_{P,dc}$ depending on the ac source or dc source, respectively. Also, $\omega = \{2\pi f_{sw}\}$ states angular operating frequency and n is the turns ratio between primary and secondary coupler coils which is indicated as $n = \sqrt{L_S}/L_P$. The system resonant frequency can be expressed by resonant compensation parameters as,

$$\begin{aligned} \omega_o &= \frac{1}{\sqrt{L_P C_{Pp1}}} = \frac{1}{\sqrt{L_S C_{Ps1}}} \\ &= \frac{1}{\sqrt{(L_P - L_{Lp}) C_{Sp1}}} = \frac{1}{\sqrt{(L_S - L_{Ls}) C_{Ss1}}} \end{aligned} \quad (16)$$

The presented structure's voltage gain function can be extracted as,

$$\begin{aligned} |M_{V,gain}| &= \left| \frac{V_O}{V_P} \right| \\ &= \left| \frac{\omega^2 L_M C_{Pp1}}{\left(1 - (\omega/\omega_o)^2 + j\omega C_{Ss1} R_{L,eq} \right) \left(1/C_{Ps1} + j\omega L_S \right) + j\omega L_{S1} + R_{L,eq}} \right| \end{aligned} \quad (17)$$

III. EXPERIMENTAL RESULTS

In order to validate the operation of the proposed system from ac grid and dc grid source, an experimental test setup was built in the laboratory as displayed in Fig. 3.



Fig. 3. The test set-up demonstration.

Parameter values of the proposed system's components are given in Table I for the experimental setup.

TABLE I – EXPERIMENTAL VALUES OF COMPONENTS

sign	component description	value
V_{ph}	ac input voltage	277 V _{AC,RMS}
V_{dc}	dc input voltage	277 V _{DC}
V_O	dc output voltage	350 V _{DC}
P_o	rated output power	20 kW
L_i	input filter inductor	1.2 mH
C_d	decoupling capacitor	2.33 μ F
L_{Ps}	primary series inductor	4.27 μ H
C_{Pp}	primary parallel capacitor	255 nF
C_{Ps}	primary series capacitor	340 nF
L_P	primary self-inductances	42 μ H
L_S	secondary self-inductances	42 μ H
C_{Ss}	secondary series capacitance	340 nF
C_{Sp}	secondary parallel capacitance	255 nF
L_{Ss}	secondary series inductor	4.27 μ H
k	coupling co-efficient	0.15
C_e	decoupling capacitor	0.34 μ F
L_C	common mode choke	150 μ H
f_{60}	grid frequency	60 Hz
f_{sw}	operating frequency	93.5 kHz
t_{dead}	dead time	600 ns

Both the primary and secondary coupler coils are identical polyphase and separated to have 6 inches ground clearance between coils. The ORC on the primary side can be operated with ac grid or dc grid input options. Resonant inverter was built with 1200V, 256A rated Wolfspeed/CREE SiC power modules in three half-bridge arrangements. In order to drive the three phase power modules, CREE gate drivers are used for the operation of the inverter. Also, rectifier diode assembly was developed using SiC Schottky GB2X50MPS17 diodes with the rating of 1700 V/168 A (per device at $T_c=75$ °C). Cooling system uses water and ethylene glycol mix. TMS320F28335PGFA DSP module from Texas Instruments is used to control the proposed converter. In the ac-to-dc power flow experiments, Ametek RS90 90 kW ac grid emulator is used

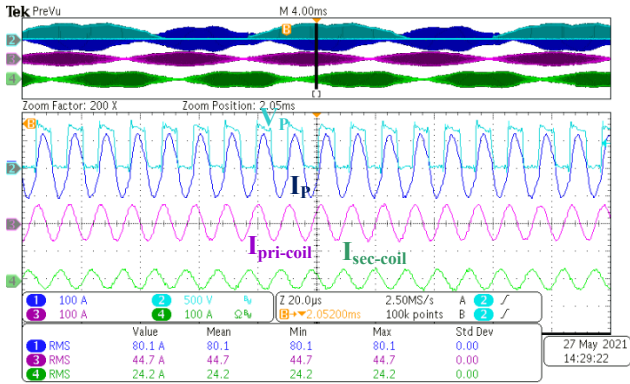


Fig. 4. The experimental results of ac-to-dc power transfer from ac grid source for 20 kW power transfer.

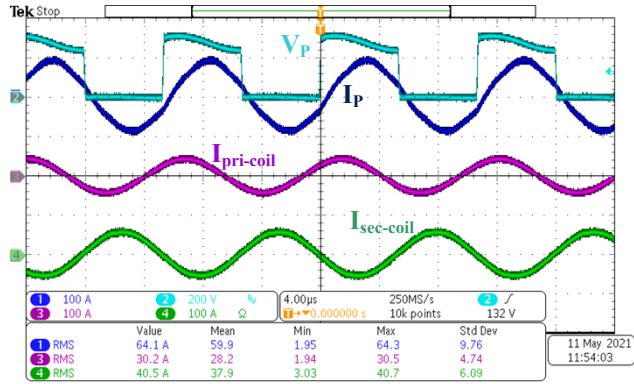


Fig. 5. The experimental results of dc-to-dc power transfer from dc grid source for 20 kW power transfer.

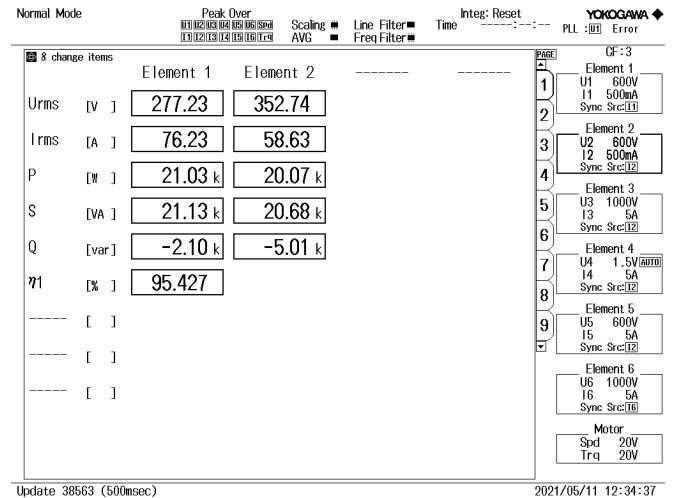
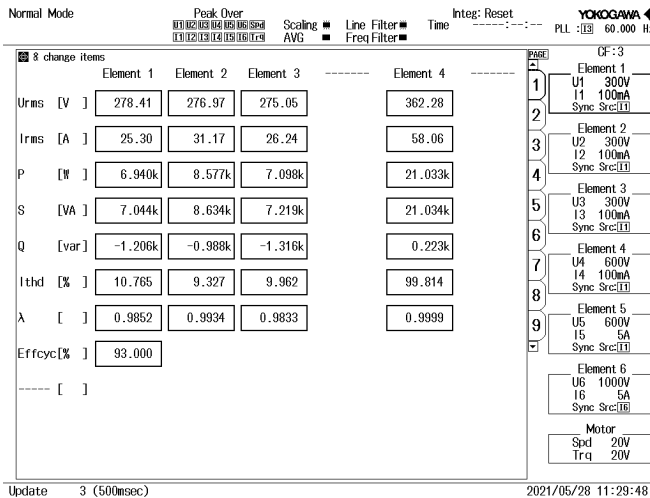


Fig. 6. The experimental results of ac-to-dc and dc-to-dc power transfer at 20 kW from a) ac grid source, b) dc grid source.

at the input of the three-phase ORC inverter. In the dc-to-dc power transfer experiment, NHR 9300 100 kW battery emulator is used. For the ac-to-dc experimental results from ac grid emulator, the resonant circuit phase voltage and current signals are shown in Fig. 4 for 20 kW power transfer to the secondary side load. The experimental results of dc-to-dc resonant circuit voltage and current waveforms are presented in Fig. 5 for 20 kW load power loads.

The numerical measurement of the experimental results is recorded using a Yokogawa WT1806E precision power analyzer as demonstrated in Fig. 6 (a) and (b). As seen from the numerical results, the system input current THD is acquired around 9-10% with 0.98-0.99 PF and overall efficiency is 93% from ac grid source to the load. Additionally, the experimental result of the system shows that an overall 95.4% efficiency is achieved from dc source to the load.

IV. CONCLUSIONS

This study presents an integrated wireless power transfer system with ORC that can be used from ac grid or dc grid source

in microgrid applications. Theoretical analysis of the proposed system is completed, and experimental results are provided for ac-to-dc and dc-to-dc operation modes. According to the experimental test results, when transferring power in ac-to-dc mode from ac grid emulator, 93% overall system efficiency is recorded at 20 kW power transfer with 9-10% grid current THD and 0.98-0.99 PF. When the operating mode is from dc battery emulator, 95.4% of overall efficiency is measured, while transferring 20 kW to the dc load terminals.

ACKNOWLEDGEMENTS

This project is funded by Oak Ridge National Laboratory's Laboratory Directed Research and Development (LDRD) Program's Transformational Energy Science and Technology (TEST) initiative with the project ID LOIS-9505. This research used resources available at the Power Electronics and Electric Machinery Research Center located at the National Transportation Research Center, a DOE EERE User Facility operated by the Oak Ridge National Laboratory (ORNL). The authors would like to thank the TEST Initiative Lead, Dr. Ilias Belharouak for his support of this work and his guidance. Authors also acknowledge the support and guidance of ORNL Sustainable Transportation Program Manager, Dr. Rich Davies, which is greatly appreciated.

REFERENCES

- [1] O. C. Onar, G. -J. Su, E. Asa, J. Pries, V. Galigekere, L. Seiber, C. White, R. Wiles, and J. Wilkins, "20-kW bi-directional wireless power transfer system with energy storage system connectivity," in *Proc., IEEE Applied Power Electronics Conference and Exposition (APEC)*, pp. 3208-3214, March 2020, New Orleans, LA.
- [2] E. Asa, O. C. Onar, V. P. Galigekere, G. -J. Su, and B. Ozpineci, "A novel bi-directional ac/dc – dc/ac wireless power transfer system for grid support applications," in *Proc., IEEE Applied Power Electronics Conference and Exposition (APEC)*, pp. 1197-1202, June 2021, Phoenix, AZ.
- [3] B. R. Ravada, N. R. Tummuru, and B. N. L. Ande, "PV-wind and hybrid energy storage integrated multi-source converter configuration based grid-interactive microgrid," *IEEE Transactions on Industrial Electronics*, vol. 68, no. 5, pp. 4004-4013, May 2021.
- [4] A. Vettuparambil, K. Chatterjee, and B. G. Fernandes, "A multiport converter interfacing solar photovoltaic modules and energy storage with DC microgrid," *IEEE Transactions on Industrial Electronics*, vol. 68, no. 4, pp. 3113-3123, Apr. 2021.
- [5] E. Asa, O. C. Onar, V. P. Galigekere, G. -J. Su, and B. Ozpineci, "A novel three-phase oak ridge ac / ac converter for wireless mobility energy storage system (WMESS) connectivity," in *Proc., IEEE Applied Power Electronics Conference and Exposition (APEC)*, pp. 758-764, June 2021, Phoenix, AZ.
- [6] E. Asa, O. C. Onar, V. P. Galigekere, R. Zheng, G. -J. Su, and B. Ozpineci, "A novel three phase Oak Ridge dc / ac converter for wireless grid tied applications," in *Proc., IEEE Transportation Electrification Conference & Expo (ITEC)*, pp. 1-6, June 2021, Chicago, IL.
- [7] E. Asa, O. C. Onar, V. P. Galigekere, G. -J. Su, and B. Ozpineci, "A novel three-phase Oak Ridge ac / dc converter for wireless EV charger applications," in *Proc., IEEE Applied Power Electronics Conference and Exposition (APEC)*, pp. 437-443, June 2021, Phoenix, AZ.
- [8] E. Asa, J. Pries, V. Galigekere, S. Mukherjee, O. C. Onar, G. -J. Su, and B. Ozpineci, "A novel ac to ac wireless power transfer system for EV charging applications," in *Proc., IEEE Applied Power Electronics Conference and Exposition (APEC)*, pp. 1685-1690, March 2020, New Orleans, LA
- [9] E. Asa, O. C. Onar, J. Pries, V. Galigekere, and G. -J. Su, "A tradeoff analysis of series / parallel three-phase converter topologies for wireless extreme chargers," in *Proc., IEEE Transportation Electrification Conference & Expo (ITEC)*, pp. 1093-1101, June 2020, Chicago, IL
- [10] A. Greifelt, B. Rubey, and D. Gerling, "High temperature superconductor based 500 kW smart grid charging for mobile applications," in *Proc., IEEE Vehicle Power and Propulsion Conference (VPPC)*, pp. 1-5, Dec. 2017, Belfort, France.
- [11] E. Asa, V. Galigekere, O. C. Onar, B. Ozpineci, J. Pries, and G. -J. Su, "Wireless Power System," U.S. Patent 2021/0188106 A1, Jun. 24, 2021. Online Available: <https://patents.google.com/patent/US20210188106A1>. Accessed on: Nov. 24, 2021.
- [12] J. Pries, V. P. N. Galigekere, O. C. Onar, G. -J. Su, "A 50-kW three-phase wireless power transfer system using bipolar windings and series resonant networks for rotating magnetic fields," *IEEE Transactions on Power Electronics*, vol. 35, no. 5, pp. 4500-4517, May 2020.